Location Dependent Allocation of Timers and Buffers at Layer-2 in LEO Based 5G-NTN

Chandan Kumar Sheemar, Sumit Kumar, Jorge Querol, Symeon Chatzinotas,
Interdisciplinary Centre for Security, Reliability and Trust (SnT), University of Luxembourg, Luxembourg,
Email:{chandan.kumar.sheemar, sumit.kumar, jorge.querol,symeon.chatzinotas}@uni.lu,

***Abstract*—The integration of Terrestrial Networks (TN) and Non-Terrestrial Networks (NTN), primarily utilizing satellites, has gained significant attention due to the potential of NTN to provide widespread coverage. The unique physical layer properties of 5G-NR offer the possibility of direct access to 5G services through satellites. However, the substantial Round-Trip Delays (RTD) associated with NTNs necessitate a re-evaluation of the design of timers and buffers in the RLC and PDCP layers. This is particularly crucial for regenerative payload satellites with limited computational resources that require optimal utilization of the available resources. This research aims to explore the integration of emerging NTNs with limited resources from a higher-layer perspective. We propose a novel and efficient method for designing the buffers and timers in the RLC and PDCP layers without the need for intensive computations. Since the optimal solution depends on the RTD, which might result to be different for users located at different spots of the satellite beam, a user location-dependent approach is adopted. This approach is particularly relevant for efficiently utilizing the available limited resources and avoiding unnecessary delays in the system. Through simulations, we demonstrate that the proposed methods significantly improve performance in terms of resource utilization and reducing delays.**

***Index Terms*—Non-Terrestrial Networks, 5G-NR, RLC, PDCP**

I. Introduction

Non-Terrestrial Networks (NTNs) refer to communication networks that operate in space, beyond the boundaries of Earth's surface [1]. These networks utilize satellites, space-based platforms, or other orbiting infrastructures to establish connectivity and enable communication services. NTNs play a crucial role in bridging the digital divide, providing global coverage, and extending connectivity to remote and underserved areas where terrestrial infrastructure is limited or absent. They are instrumental in supporting various applications, including telecommunications, internet access, broadcasting, and disaster response, by leveraging the advantages of satellite-based communication systems in terms of wide coverage, mobility, and scalability [2].

However, compared to the conventional Terrestrial Networks (TNs) [3]–[6], NTNs suffer from additional challenges due to extremely large round-trip delays (RTDs) for Geosynchronous Earth Orbits (GEO), Medium Earth Orbit (MEO) and Low Earth Orbit (LEO) satellites [7], [8]. Nonetheless, the benefits of NTN have motivated the 3GPP, which has been otherwise involved in the standardisation of TN communications only, to take a big leap towards studying the issues and providing solutions for integrating NTN in the 5G ecosystem [9]. From 3GPP Release 17 onwards, satellites have become an integral part of the 5G deployment [10], [11], and this integration is coined as 5G-NTNs.

In 3GPP Release 17, significant emphasis was placed on transparent payloads, aiming to facilitate direct access to 5G services for user equipment (UEs) situated on Earth. Satellites equipped with transparent payloads are advantageous due to their cost-effectiveness, as they primarily serve as signal amplifiers and forwarders between ground-based gNBs and UEs. Essentially, they function as high-altitude relays, enabling long-distance communication between distant entities on Earth. This straightforward setup maximizes the utilization of the existing satellite fleet while allowing both the gNB and UE to operate on the ground.

Conversely, regenerative payload satellites offer advanced capabilities, executing complex signal processing tasks tailored to specific service requirements. These satellites integrate the functionalities of a ground-based gNB, delivering substantial advantages. Nevertheless, the deployment of regenerative payload systems entails considerable additional expenses compared to transparent satellite systems. Despite this, their adoption remains highly desirable due to their potential to enable a diverse range of new services and applications while reducing RTD by half through onboard signal processing [12]. Additionally, such payloads hold promise for facilitating Inter-Satellite Links (ISLs), enhancing satellite network flexibility and agility by enabling dynamic reconfiguration and efficient resource allocation. However, the realization of regenerative payload-based 5G-NTNs is still in the early stages of research. While they bring forth new opportunities, they also present unique challenges that demand substantial collaborative efforts from academia and industry. Building such networks will necessitate innovative approaches and novel thinking in terms of system design.

The NTNs radio interface consists of four primary user-plane protocol layers for secure and reliable data transfer between the UE and gNB. Such layers, which are part of the protocol stack of both the UE and gNB, are the following: 1) Physical (PHY) layer, 2) Medium Access Control (MAC) layer, 3) Radio Link Control (RLC) layer, and 4) Packet Data Convergence Protocol (PDCP) layer. Several works on PHY and MAC layers are already available in the literature, and in this work, we focus on the RLC and PDCP layers, for which

only limited contributions are available.

The PDCP layer is responsible for maintaining data integrity and confidentiality. It performs tasks like compressing headers, eliminating duplicate data, and ensuring correct data order. The layer relies on mechanisms such as discard timers, transmit buffers, and reordering timers. The discard timer keeps track of how long each data unit stays in the PDCP layer and discards it if needed. The reordering timer ensures packets are delivered in the correct order at the receiver's end. The transmission buffer stores data for wireless transmission, allowing for the retransmission of lost packets. Inefficient discard timer values can lead to high memory usage and delays. Optimal discard timer values reduce memory requirements and unnecessary delays, enabling low-latency solutions for NTNs. However, solutions for their optimization are not available yet in the literature.

The RLC layer ensures reliable data transmission and operates in three modes: transparent mode (TM), unacknowledged mode (UM), and acknowledged mode (AM). RLC-TM passes data without adding reliability mechanisms, suitable for streaming applications. RLC-UM sends data without waiting for acknowledgements, suitable for applications tolerant of some packet loss. RLC-AM uses reliability mechanisms like segmentation, retransmission, and status reporting for high-reliability applications. For NTNs, significant challenges arise in RLC-AM due to its retransmission mechanism. The reassembly timer in AM ensures packets are received in order. Adjusting reassembly timer values carefully prevents unnecessary delays and degradation of throughput/rate at higher layers. Also, solutions for optimizing such a parameter remain unexplored in the literature.

A. Motivation and Main Contributions

In [13], we presented a hardware demonstrator with hard-coded RLC and PDCP parameters for 5G-NTNs. However, It is noteworthy that such parameters are intricately connected to the RTD and the effective number of retransmissions required in the system. In [14], we presented the first ever contribution for RLC and PDCP layers. However, such work was limited to a single user, with any consideration regarding its position withtin the satellite beam.

However, in a general setting, the RTD experienced by each user in the network depends significantly on their relative position in relation to the satellite. Additionally, the number of retransmissions needed is influenced by the effective channel conditions between the user and the satellite. Figure (1) visually illustrates the relationship between user position, RTD, and the number of retransmissions. We can see that users in different circles experience different RTDs due to different path-loss. Furthermore, the number of retransmissions is affected due to and different signal-to-noise ratio (SNR) levels at the PHY layer, due to large variation in the distances. The observed variation in RTDs and the number of retransmissions emphasizes the necessity of an adaptive approach that takes into account the user's location when fine-tuning the parameters for optimal performance. To address this

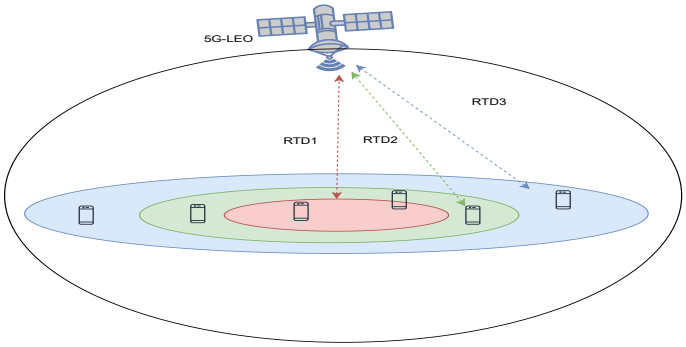

Fig. 1: 5G-LEO satellite serving multiple users with different RTD zones.

requirement, a cluster-dependent approach can be employed, where users located at the same distance from the center of the beam are grouped together in clusters and independent optimization takes place for each cluster. Within a specific cluster, the RLC and PDCP parameters can be jointly tuned since the RTD values and SNR levels at the PHY layer are approximately similar for users within the cluster. However, when the users move to another cluster, the solution must be readapted.

In this work, we embark on the task of formulating an adaptive solution to address the dynamic characteristics of RLC and PDCP parameters, while accounting for the varying impact of RTD and distinct retransmission requirements inherent to each user cluster. Our methodology commences by constructing a sophisticated multi-parameter estimator meticulously designed to ascertain the precise retransmission thresholds necessary for optimal performance within each user cluster. Subsequently, we engage in an in-depth analysis of the RLC layer, where we derive tailored buffer size configurations for each cluster, with the overarching objective of minimizing latency and maximizing data throughput. To further refine our adaptive solution, we undertake the optimization of timer parameters within the RLC and PDCP layers, striving to strike an equilibrium that optimizes communication performance, reliability, and responsiveness for each specific user cluster.

II. System Model and Solutions

We consider a multi user setup in which multiple users are available in the LEO satellite beam. We assume that the area covered by the satellite beam to be divided into C clusters, with users located in one particular cluster having the same RTD. Let $\mathcal{C}$ denotes the set containing the indices of these clusters. We consider two categories: 1) The computational resources to be independent per cluster, such that the optimizaiton can be carried out per cluster basis; 2) The computational resources are shared for all users, and optimization is carried out jointly to find the parameters which satisfy the overall requirements.

A. PDCP Layer Optimization

1) PDCP Discard Timer*:* Let t_d^c, with $c \in \mathcal{C}$ denote the discard timer for the PDCP layer for cluster c, which is typically configured for each data radio bearer (DRB). Upon receiving the service data unit (SDU) from the radio resource layer (RRC), the PDCP entity initiates a timer to monitor its stay duration within the transmission buffer. The PDCP entity discards the PDCP SDU either when the timer for each SDU surpasses the specified discard timer value (t_d^c) or when it receives confirmation of the correct reception of the PDCP SDU to the users within cluser $c \in \mathcal{C}$.

In our efforts to optimize the value of t_d^c for cluster c, we propose a periodic adaptation mechanism over a specified time interval of T_d^c. During this period, we monitor the system for a brief duration of T_o^c, during which we accurately receive and confirm the reception of a specific number of packets O^c from cluster c, including any retransmissions. To achieve this, we leverage time stamps (TS) associated with each SDU received from the upper layer from cluster c, enabling us to fine-tune t_d^c, $\forall c$.

We initiate this process by initially setting t_d^c to a large value, often following 3GPP recommendations, which typically range from $1000 - 1500$ milliseconds [10], [11]. We maintain a set $\mathcal{T}_d^c = \{t_0^c, t_1^c, ..., t_O^c\}$ containing the indices of the TSs for the first O SDUs that are correctly received during this period. Note that this contains the observations of the correctly received packets from all the users within cluster c. It is important to note that during this timeframe, we discard packets from the transmission buffer only when the peer PDCP entity successfully receives them. However, it is possible that some packets may be received correctly at the receiver during the timer T_d^c, but their acknowledgments (ACKs) are lost. In such cases, we exclude the TSs of these packets from the set $\mathcal{T}_d^c$, as they may provide inaccurate estimates of the effective number of retransmissions.

Let r_d^c represent the round-trip delay experienced by the 5G-LEO satellite between the PHY layer for cluster c. From the perspective of the PDCP layer, the discard timer value t_d^c assigned to cluster c can be expressed as $t_d^c = N^c \ (r_d^c + 4(t_{pro}^{PDCP} + t_{pro}^{RLC} \ + \ t_{pro}^{L}))$, where N^c is a positive integer representing a multiple of the RTD times the actual number of retransmissions that occurred for cluster c. Additionally, constants t_{pro}^{PDCP} and t_{pro}^{RLC} denote the processing time delays at the PDCP and RLC layers, respectively, while t_{pro}^{L} accounts for the overall processing delay at the lower layers, including aspects like modulation, demodulation, encoding, decoding, medium access control, flow control, compression/decompression, data ciphering/deciphering, packet reordering, header removal, and more. The scalar value 4 accounts for the path from the transmitter to the receiver, spanning up to the PDCP layer, and the return path from the receiving PDCP entity to the transmitting one, leading to a fourfold experience of the processing delay (t_{pro}^{PDCP}+t_{pro}^{RLC} + t_{pro}^{L}). Notably, these constants are inherent to the regenerative payload system and are readily known at the systems level, and we assume them to be the same for each cluster. Importantly, the average effective number of retransmissions required, as seen from the PDCP layer perspective, may fluctuate depending on channel conditions and SNR. Therefore, it is essential to accurately estimate this value to adapt t_d^c appropriately.

Remark: In the case when a joint optimization for this parameter is required, the maximum number of retransmissions within the entire beam in the LEO satellite is required.

Consider examining the packets observed along with their associated time stamps in $\mathcal{T}_d^c$ in cluster $c \in \mathcal{C}$. Our objective here is to derive an estimate for the maximum number of retransmissions for cluster c, based on the observations, allowing us to set the discard timer value as precisely as feasible in line with the actual retransmission occurrences within the NTN system. We can determine this maximum number of retransmissions by solving the following optimization problem using the data from $\mathcal{T}_d^c$.

$$\max_{t^c} \quad \frac{t^c - 4(t_{pro}^{PDCP} + t_{pro}^{RLC} \ + \ t_{pro}^{L})}{r_d} \tag{1a}$$

$$\text{s.t.} \quad t^c \in \mathcal{T}_d \tag{1b}$$

This problem can be readily addressed by examining the durations that the O^c packets have spent in the buffer, as recorded in $\mathcal{T}_d^c$. We can easily obtain the optimal solution, denoted as $t_d^{c^*}$, for (1). An estimator for determining the effective maximum number of retransmissions N^c can be obtained as follows:

$$N^c = \lceil \frac{t_d^{c^*} - 4(t_{pro}^{PDCP} + t_{pro}^{RLC} \ + \ t_{pro}^{L})}{r_d} \rceil \tag{2}$$

where $\lceil \cdot \rceil$ denotes the least greatest integer.

It is important to highlight that the proposed solution remains applicable up to a specific time point, denoted as T_D^c, during which we assume a constant value for r_d^c. However, as the satellite's position shifts, the propagation delay naturally fluctuates. Consequently, it becomes necessary to readjust the discard timer value by observing the O^c TSs within the new time interval. This observation enables us to estimate the system's maximum number of retransmissions effectively occuring in each cluster.

In case the resources are shared in the LEO satellite, in such a case, let $\mathbf{N} = [N^1, ..., N^C]$ denote the estimators for the number of transmission in each cluster. The joint timer for all the cluster can be set as

$$N = max \ \ \mathbf{N}, \tag{3}$$

which selects the maximum value of $\mathbf{N}$, thus accounting for the maximum number of retransmissions occurring in the system for the worst case user, denoted as N.

The complete procedure for creating an adaptive estimator to ascertain the maximum retransmission count per cluster within the system is delineated in Figure 2. This estimation can subsequently be employed to determine the ideal setting for the discard timer per cluster. In the case of shared resources, one the procedure above has been executed per cluster,

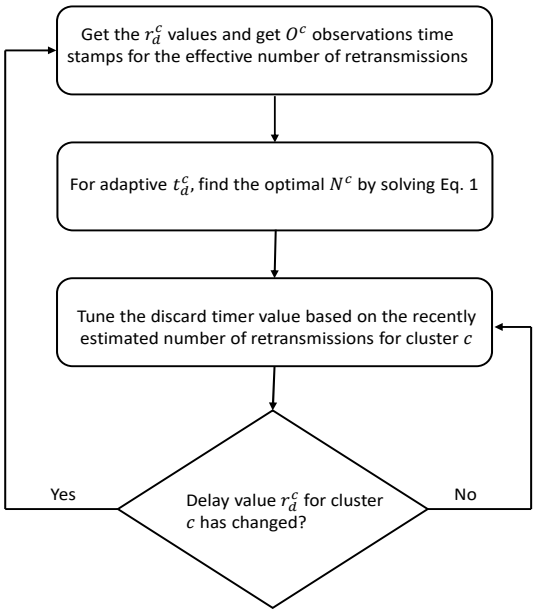

Fig. 2: Flowchart of the adaptive estimator of the discard timer value.

2) PDCP Transmit Buffer: The buffer size within the PDCP layers holds significant importance in the next-generation NTNs, especially in compact and cost-effective setups. The reason for this lies in the substantial propagation delays, which can lead to a rapid accumulation of packets awaiting ACK. As a result, this situation places rigorous requirements on ample memory capacity, potentially driving up the costs associated with NTNs considerably.

The optimization of the transmit buffer hinges on two key factors: the system's throughput from the perspective of the PDCP layer at the transmission end and the time required to receive ACKs confirming the correct reception of packets, which allows for the release of a portion of the memory. This consideration encompasses both the RTD and the number of retransmissions N^c for cluster c occurring at the lower layers. Specifically, let R_p^c represent the effective rate at the PDCP layer, which the transmit buffer needs to support to prevent packet loss for cluster c, resulting into cluster throughput. This rate is denoted as the number of packets transmitted from the PDCP layer within one millisecond within cluster c. The effective number of retransmissions within the system has been estimated when optimizing the discard timer value, as indicated in (2). To determine the optimal buffer size to support the cluster throughput, we must calculate the total number of packets that will be stored as copies in the transmit buffer when the effective transmission rate is R_p^c. Let P^c denote the number of packets to be accommodated in the buffer allocated to cluster c. It can be demonstrated that the number of packets transmitted over time while awaiting ACKs for these packets is expressed as:

$$P^c = N^c \left(r_d^c + 4(t_{pro}^{PDCP} + t_{pro}^{RLC} + t_{pro}^{L})\right) R_p^c. \quad (4)$$

In the case of shared memory, the optimal buffer size to support the system throughput, instead of the cluster throughput, needs to be computed. This can be computed as

$$P = \sum_{c \in \mathcal{C}} P^c, \quad (5)$$

thus considering the total number of packets in the system.

Assuming that each memory cell of the buffer can accommodate one packet, (4) serves as a representation of the minimal buffer size, denoted as $B^{c^*} = P^c$, in terms of the required memory cells needed to sustain the throughput R_p^c for cluster $c \in \mathcal{C}$ without encountering packet loss within the 5G-NTN system. Should the chosen buffer size be smaller than $P^c = B^{c^*}$, it would lead to packet loss directly at the transmitter, prompting higher layers to reduce the packet rate. It is worth noting that the optimal buffer size is contingent on the RTD value $r_d^c, \forall c \in \mathcal{C}$. Consequently, as the regenerative payload changes position, both the RTD value and the optimal buffer size undergo changes for each cluster. Therefore, this proposed solution allows for the dynamic allocation of the minimum memory required by 5G-NTNs to support the desired throughput or effective rate R_p^c. In the case of shared memory, the optimal buffer size can be computed based on the total number of packets transmitted in the system, given as $P = B^*$.

In cases where the RTD is substantial, a significant memory portion is reserved for storing packet copies. However, as the satellite orbits closer to Earth, the RTD diminishes, freeing up a substantial portion of memory that can be repurposed for other uses.

3) PDCP Reordering Timer*:* Let us introduce the reordering timer, denoted as t_r^c, which serves as a crucial element within the PDCP layer at the receiving end. Its primary function is to ensure that packets are delivered to the upper layers of the protocol stack in the correct sequence. When a packet is transmitted over the air interface, it can undergo delays or arrive out of order due to various factors, such as network congestion or interference. Upon reception by the PDCP layer, each packet is assigned a sequence number (SN) based on its order of transmission. The PDCP layer then compares the SN of each received packet to the expected SN. If the received packet's SN is lower than the expected SN, it is considered an out-of-order packet and is temporarily stored in the reordering buffer. The reordering timer comes into play when the first out-of-order packet is received, and its value is determined based on the anticipated delay for the missing packet to arrive.

Our proposed approach addresses this challenge by leveraging information obtained from the initial O^c samples for each cluster c. Initially, we set the values to their maximum as per the 3GPP solution. However, as different received packets may exhibit varying delay values, our goal is to extract information regarding the maximum number of retransmissions observed at the receiver based on this observational data.

It is essential to note that on the receiver side, only half of the RTD is experienced compared to the transmitting PDCP

entity, as the receiver does not need to wait for acknowledgement. Thus, we represent this reduced propagation delay as $r_d/2$.

The expected delay to receive packets in cluster c at the PDCP receiver entity, accounting for retransmissions and processing delays at the lower layers, can be expressed as:

$$t_r^c = M^c(r_d/2 + 2(t_{pro}^{PDCP} + t_{pro}^{RLC} + t_{pro}^{L})), \tag{6}$$

The term $r_d/2$ accounts for the precise propagation delay experienced from the transmitter to the receiver at the PHY layer, while M^c represents the effective number of retransmissions. It is important to note that the count of effective retransmissions observed at the receiver may differ from N^c or N in the case of shared memory. This disparity primarily arises because a packet can be received correctly at the PDCP layer, but its ACK may be lost. In such instances, the transmitter will retransmit the packets for which no ACK is received, even though they will ultimately be discarded at the receiver's end. Therefore, the estimation of M^c needs to be carried out separately by the entities situated on the ground in cluster c.

To establish an estimator for determining the maximum number of retransmissions occurring within the system, we must estimate and address the following optimization problem based on our observations:

$$\max_{t^c} \quad \frac{t^c - 2(t_{pro}^{PDCP} + t_{pro}^{RLC} + t_{pro}^{L})}{r_d/2} \tag{7a}$$

$$\text{s.t.} \quad t \in \mathcal{T}_r^c \tag{7b}$$

In this context, $\mathcal{T}_r^c$ represents a set containing the O^c TSs observed at the receiver, encompassing correctly received packets, including retransmissions. Solving this problem becomes straightforward by comparing the ratio defined in (7a) with t^c assessed using the observation data within $\mathcal{T}_r^c$. Let us denote the optimal solution for problem (7) as $t_r^{c^*}$. With this in place, we can determine the maximum expected number of retransmissions within the system as follows:

$$M^c = \lceil \frac{t_r^{c^*} - 2(t_{pro}^{PDCP} + t_{pro}^{RLC} + t_{pro}^{L})}{r_d/2} \rceil \tag{8}$$

In the case of shared resources in the LEO satellite, $\mathbf{M} = [M^1, ..., M^C]$ denote the estimators for the number of transmissions in each cluster. The joint timer values for all the clusters can be set as

$$M = max \ \mathbf{M}, \tag{9}$$

which selects the maximum number of retransmissions for the worst-case user.

B. RLC Layer Optimization

The RLC layer in acknowledged mode (RLC AM) plays a crucial role in ensuring reliable data transfer between the NTN wireless interface and the core network. Its responsibilities encompass tasks such as data segmentation and reassembly, error correction, and flow control. Positioned above the physical layer, the RLC layer provides essential services to upper-layer protocols. Notably, the RLC layer faces a significant challenge, particularly on the receiver side, due to the presence of substantial RTDs. Specifically, it relies on the reassembly timer t_{re}^c as a critical parameter to ensure the timely reception of all RLC protocol data units (PDUs) associated with a specific RLC service data unit (SDU) in cluster c. Upon receiving an RLC PDU, it is temporarily stored in a reassembly buffer until all PDUs belonging to the same RLC SDU are received. If an RLC PDU is lost or corrupted during transmission, the RLC layer initiates a retransmission request for the affected PDU. The reassembly timer begins when the first RLC PDU tied to an RLC SDU arrives and is set based on the anticipated delay for all PDUs linked to that particular RLC SDU. If all PDUs are not received within the timer's duration, the RLC layer will discard the incomplete RLC SDU.

Given our earlier estimation of the effective maximum time required to receive a packet, contingent on the scalar M^c for cluster c, the necessary time remains identical, except for the processing time at the PDCP layer, situated atop the RLC layer. Consequently, we can achieve optimal tuning of the timer t_{re}^c as follows:

$$t_{re}^c = M^c(r_d/2 + 2(t_{pro}^{RLC} + t_{pro}^{L})), \tag{10}$$

In the case of shared memory, such a formula can be recomputed based on M, considering the worst case user, leading to the computaion

$$t_{re} = M(r_d/2 + 2(t_{pro}^{RLC} + t_{pro}^{L})). \tag{11}$$

It is worth noting that buffer optimization is not a necessity for ground-based UEs, as they possess ample memory capacity to accommodate extensive data storage needs. Nonetheless, should the need arise, a comparable problem to (4) can be addressed to determine the optimal buffer size.

III. Simultaion Results

In this section, we present simulation results aimed at assessing the performance of our proposed adaptive timer and buffer approach. Our evaluation focuses on a scenario involving a single 5G LEO regenerative satellite serving multiple terrestrial UEs. We assume the geographical area to be divided into 2 clusters, with each cluster containing 2 users. For the inner cluster, the user are assumed to be located in the center of the beam and in the outer cluster, the users are assumed to be located at the edge of the beam. The LEO satellite is assumed to be operating at an altitude of 1200 kilometers and an elevation angle of 10° degrees. The RTD for the inner and the outer cluster is assumed to be 15 ms and 20 ms, respectively. Furthermore, we assume that the effective number of retransmissions observed both at the transmitter and receiver, remains consistent, i.e., $N = M$ in the case of shared memory or $N^c = M^c$ in the case of per cluster resource allocation. Such numbers are presumed to follow a uniform distribution within the interval $[\mu - 3, \mu + 4]$, where μ represents the average number of retransmissions. Therefore, higher values of μ emphasize a

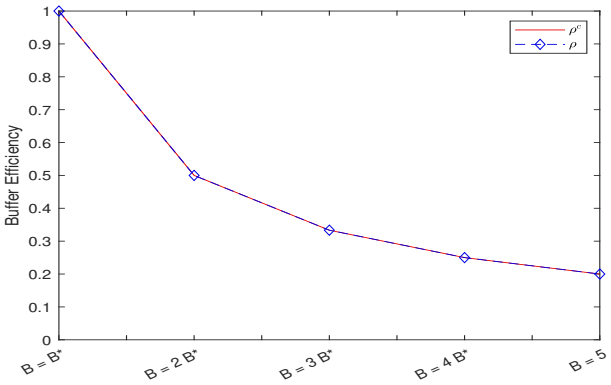

Fig. 3: PDCP Buffer efficiency as a function of the buffer size.

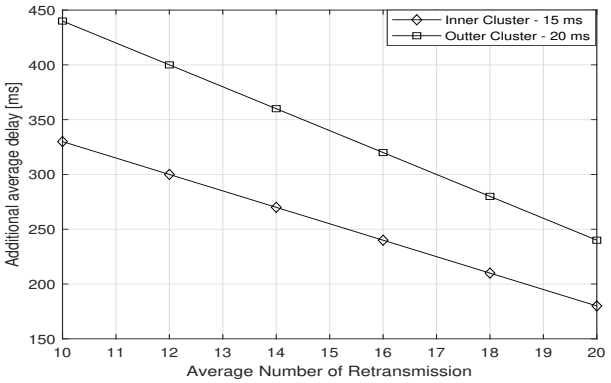

Fig. 4: Average additional delay experienced by the packet which requires retransmission but its ACK is lost.

larger number of retransmissions. The total processing delay is assumed to be $t_{pro}^{PDCP} + t_{pro}^{RLC} + t_{pro}^{L} = 0.5$ ms. We assume that for each cluster should support the cluster rate of $R_p^1 = R_p^2 = 10\ pck/ms$. For the case for which shared memory is allocated, the total system throughput assumed to be supported is $R = 20\ pck/ms$. The maximum number of retransmissions is set to 32.

To evaluate the accuracy of the optimal buffer size, we define the following metrics

$$\rho = \rho^c = \frac{\text{Number of packets filled in the buffer}}{\text{total buffer size}} \tag{12}$$

where ρ and ρ^c denote the buffer efficiency of shared memory case and joint allocation case.

Fig. 3 highlights the buffer efficiency at the PDCP layer as a function of the buffer size which is chosen to be a multiple of the optimal buffer size computed according to the proposed solution. It is clearly visible that the proposed solution provides the highest buffer efficiency and results in the minimum buffer size to support the desired throughput in the two cases.

Figure 4 illustrates the average added delay experienced by a packet needing retransmission when its ACK is lost. We show the case of two circles with two different RTD, i.e., 15 ms and 20 ms. This delay is depicted as a function of the average number of retransmissions μ under the worst-case scenario with a maximum number of retransmissions, as opposed to the adapted solution proposed in this study. It is evident that packets requiring retransmission with their ACKs being lost face significant delays, particularly when the effective number of retransmissions in the system is minimal but the packets are forced to wait for the maximum time before being transmitted. However, our cluster-based solution exhibits superior performance as it is able to adapt on RTD basis. On the other hand, if collective solution is desirable in the case of shared memory, the packets will wait longer before being transmitted.

IV. Conclusions

This paper proposed a novel strategy to optimize the RLC and PDCP layers for NTNs based on location dependence. Due to different RTDs in the same beam, the proposed solution enables to optimization of the timers and buffers in the NTN systems on a cluster basis with users belonging to each cluster having the same RTD. Simulation results validate the performance gains of the proposed approach, both in terms of buffer efficiency and smaller waiting times.

Acknowledgment

5G-LEO is funded under the ESA ARTES program with ESA Contract No. 4000135152/21/NL/FGL. [1]

References

[1] O. Kodheli, A. Guidotti, and A. Vanelli-Coralli, "Integration of satellites in 5g through leo constellations," in *IEEE GLOBECOM*, 2017, pp. 1–6.
[2] M. Giordani and M. Zorzi, "Non-terrestrial networks in the 6G era: Challenges and opportunities," *IEEE Network*, vol. 35, no. 2, pp. 244–251, 2020.
[3] C. K. Sheemar, C. K. Thomas, and D. Slock, "Practical hybrid beamforming for millimeter wave massive MIMO full duplex with limited dynamic range," *IEEE OJ-COMS*, vol. 3, pp. 127–143, 2022.
[4] C. K. Sheemar and D. Slock, "Hybrid beamforming for bidirectional massive MIMO full duplex under practical considerations," in *IEEE VTC2021-Spring*, 2021, pp. 1–5.
[5] ——, "Receiver design and agc optimization with self interference induced saturation," in *IEEE ICASSP*, 2020, pp. 5595–5599.
[6] C. K. Thomas, C. K. Sheemar, and D. Slock, "Multi-stage/hybrid bf under limited dynamic range for OFDM FD backhaul with MIMO si nulling," in *2019 16th International Symposium on Wireless Communication Systems (ISWCS)*. IEEE, 2019, pp. 96–101.
[7] M. Höyhtyä, S. Boumard, A. Yastrebova, P. Järvensivu, M. Kiviranta, and A. Anttonen, "Sustainable satellite communications in the 6G era: A european view for multi-layer systems and space safety," *IEEE Access*, 2022.
[8] V. M. Baeza, E. Lagunas, H. Al-Hraishawi, and S. Chatzinotas, "An overview of channel models for ngso satellites," in *IEEE VTC2022-Fall*, 2022, pp. 1–6.
[9] M. M. Azari, S. Solanki, S. Chatzinotas, O. Kodheli, H. Sallouha, A. Colpaert, J. F. M. Montoya, S. Pollin, A. Haqiqatnejad, A. Mostaani *et al.*, "Evolution of non-terrestrial networks from 5G to 6G: A survey," *IEEE communications surveys & tutorials*, 2022.
[10] "3GPP TR 38.811, "3rd Generation Partnership Project; Technical Specification Group Radio Access Network; Study on New Radio (NR) to support non terrestrial networks (Release 15)"," 2019.
[11] "3GPP TR 38.821, "3rd Generation Partnership Project; Technical Specification Group Radio Access Network; Solutions for NR to support non-terrestrial networks (NTN) (Release 16)"," 2021.
[12] G. Araniti, A. Iera, S. Pizzi, and F. Rinaldi, "Toward 6G non-terrestrial networks," *IEEE Network*, vol. 36, no. 1, pp. 113–120, 2021.
[13] S. Kumar, A. K. Meshram, A. Astro, J. Querol, T. Schlichter, G. Casati, T. Heyn, F. Völk, R. T. Schwarz, A. Knopp *et al.*, "Openairinterface as a platform for 5g-ntn research and experimentation," in *IEEE FNWF*, 2022, pp. 500–506.
[14] C. K. Sheemar, S. Kumar, J. Querol, and S. Chatzinotas, "Adaptive timers and buffer optimization for layer-2 protocols in 5g non-terrestrial networks," *arXiv preprint arXiv:2308.09809*, 2023.

[1] The views expressed herein can in no way be taken to reflect the official opinion of the European Space Agency